

The pseudo-spin symmetry in Zr and Sn isotopes from the proton drip line to the neutron drip line

J. Meng^{*,a,b}, K.Sugawara-Tanabe^{a,c}, S.Yamaji^a, and A.Arima^a

**Department of Technical Physics, Peking University,*

Beijing 100871, P.R. China

^a The Institute of Physical and Chemical Research (RIKEN)

Hirosawa 2-1, Wako-shi, Saitama, 351-0198 JAPAN

^bInstitute of Modern Physics, Chinese Academy of Sciences

Lanzhou 730000, China

^c Otsuma Women's University, Tama, Tokyo 206-8540, Japan

September 14, 2018

Abstract

Based on the Relativistic continuum Hartree-Bogoliubov (RCHB) theory, the pseudo-spin approximation in exotic nuclei is investigated in Zr and Sn isotopes from the proton drip line to the neutron drip line. The quality of the pseudo-spin approximation is shown to be connected with the competition between the centrifugal barrier (CB) and the pseudo-spin orbital potential (PSOP). The PSOP depends on the derivative of the difference between the scalar and vector potentials dV/dr . If $dV/dr = 0$, the pseudo-spin symmetry is exact. The pseudo-spin symmetry is found to be a good approximation for normal nuclei and to become much better for exotic nuclei with highly diffuse potential, which have $dV/dr \sim 0$. The energy splitting of the pseudo-spin partners is smaller for orbitals near the Fermi surface (even in the continuum) than the deeply bound orbitals. The lower components of the Dirac wave functions for the pseudo-spin partners are very similar and almost equal in

magnitude.

PACS numbers : 21.10.Hw, 21.60.-n, 21.10.PC, 21.60.Jz, 27.60.j

1. Introduction

In a recent letter¹, by relating the pseudo-spin symmetry back to the Dirac equation through the framework of Relativistic Continuum Hartree-Bogoliubov (RCHB) theory², the pseudo-spin approximation in real nuclei was discussed. From the Dirac equation, the mechanism behind the pseudo-spin symmetry was studied and the pseudo-spin symmetry was shown to be related with the competition between the centrifugal barrier (CB) and the pseudo-spin orbital potential (PSOP), which is mainly decided by the derivative of the difference between the scalar and vector potentials. With the scalar and vector potentials derived from a self-consistent RCHB calculation, the pseudo-spin symmetry and its energy dependence have been discussed¹. Here we will extend our previous investigation¹ to exotic nuclei. The pseudo-spin symmetry approximation for exotic nuclei is investigated for Zr and Sn isotopes ranging from the proton drip line to the neutron drip line. The isospin and energy dependence of the pseudo-spin approximation are investigated in detail.

The concept of pseudo-spin is based on the experimental observation that the single particle orbitals with $j = l + 1/2$ and $j = (l + 2) - 1/2$ lie very close in energy and can therefore be labeled as pseudo-spin doublets with quantum number $\tilde{n} = n - 1$, $\tilde{l} = l - 1$, and $\tilde{s} = s = 1/2$. This concept was originally found in spherical nuclei 30 years ago^{3,4}, but later proved to be a good approximation in deformed nuclei as well⁵. It is shown that the pseudo-spin symmetry remains an important physical concept even in the case of triaxiality⁶.

Since the suggestion of the pseudo-spin symmetry, much efforts has been made to understand its origin. Apart from the rather formal relabeling of quantum numbers, various proposals for an explicit transformation from the normal scheme to the pseudo-spin scheme

have been made in the last twenty years and several nuclear properties have been investigated in this scheme⁷⁻¹¹. Based on the single particle Hamiltonian of the oscillator shell model the origin of pseudo-spin was proved to be connected with the special ratio in the strength of the spin-orbit and orbit-orbit interactions^{12,10} and the unitary operator performing a transformation from normal spin to pseudo-spin space was discussed¹⁰⁻¹⁴. However, it was not explained why this special ratio is allowed in nuclei. The relation between the pseudo-spin symmetry and the relativistic mean field (RMF) theory¹⁵ was first noted in Ref.⁹, in which Bahri et al found that the RMF explains approximately the strengths of spin-orbit and orbit-orbit interactions in the non-relativistic calculations. In a recent paper Ginocchio took a step further and revealed that pseudo-orbital angular momentum is nothing but the “orbital angular momentum” of the lower component of the Dirac wave function¹⁶. He also built the connection between the pseudo-spin symmetry and the equality in the scalar and vector potentials^{16,17}.

To understand to what extent it is broken in real nuclei, some investigation along this line has been done for square well potentials¹⁶ and for spherical solutions of the RMF equations¹⁸. By relating the pseudo-spin symmetry back to the Dirac equation through the framework of RCHB theory, the pseudo-spin approximation in real nuclei was shown to be connected with the competition between the centrifugal barrier (CB) and the pseudo-spin orbital potential (PSOP), which is mainly decided by the derivative of the difference between the scalar and vector potentials. With the scalar and vector potentials derived from a self-consistent Relativistic Hartree-Bogoliubov calculation, the pseudo-spin symmetry and its energy dependence have been discussed in Ref.¹.

The highly unstable nuclei with extreme proton and neutron ratio are now accessible with the help of the radioactive nuclear beam facilities. The physics connected with the extreme neutron richness in these nuclei and the low density in the tails of their distributions have attracted more and more attention not only in nuclear physics but also in other fields such as astrophysics^{19,20}. New exciting discoveries have been made by exploring hitherto inaccessible regions in the nuclear chart. It is very interesting to investigate the pseudo-spin

symmetry approximation both in normal and exotic nuclei. For this purpose, we will use the RCHB theory, which is the extension of the RMF and the Bogoliubov transformation in the coordinate representation, and provides not only a unified description of the mean field and pairing correlation but also the proper description for the continuum and its coupling with the bound state^{2,21}. As this theory takes into account the proper isospin dependence of the spin-orbit term, it is able to provide a good description of global experimental data not only for stable nuclei but also for exotic nuclei throughout the nuclear chart². It is very interesting to examine the pseudo-spin symmetry approximation in exotic nuclei, in which the mean field potentials are expected to be highly diffuse.

Recently, by relating the pseudo-spin symmetry back to the Dirac equation through the framework of RCHB theory, the pseudo-spin approximation in real nuclei was discussed. The mechanism behind the pseudo-spin symmetry was studied and the pseudo-spin symmetry was shown to be connected with the competition between the CB and the PSOP, which is mainly decided by the derivative of the difference between the scalar and vector potentials. With the scalar and vector potentials derived from a self-consistent RHB calculation, the pseudo-spin symmetry and its energy dependence have been discussed¹. Here we will extend the previous investigation to the case of exotic nuclei. The pseudo-spin splitting in Zr and Sn isotopes has been studied from the proton drip line to the neutron drip line. The energy splitting of the pseudo-spin partners, their energy and isospin dependence will be addressed. An outline of the RCHB formalism is briefly reviewed in Sec. II. In Sec. III, the Dirac equation and the formalism leading to the pseudo-spin symmetry is presented. The energy splitting of the pseudo-spin partners and its energy dependence are given in Sec. IV. The pseudo-spin orbital potential, which breaks the pseudo-spin symmetry will be studied in Sec. V. In Sec. VI, the wave-function of pseudo-spin partners will be studied. A brief summary is given in the last section.

2. An outline of RCHB Theory

The RCHB theory is obtained by combining the RMF and the Bogoliubov transformation in the coordinate representation²¹, and its detailed formalism and numerical solution can be found in Ref.² and the references therein. The RCHB theory can give a fully self-consistent description of the chain of Lithium isotopes²¹ ranging from ⁶Li to ¹¹Li. The halo in ¹¹Li has been successfully reproduced in this self-consistent picture and excellent agreement with recent experimental data is obtained. The contribution from the continuum has been taken into account and proved to be crucial to understand the halo in exotic nuclei. Based on the RCHB, a new phenomenon "Giant Halo" has been predicted. The "Giant Halo" is composed not only of one or two neutrons, as is the case in the halos in light *p*-shell nuclei, but also up to 6 neutrons²². The development of skins and halos and their relation with the shell structure are systematically studied with RCHB in Ref.²³, where both the pairing and blocking effect have been treated self-consistently. Therefore the RCHB theory is very suitable for the examination of the pseudo-spin approximation in exotic nuclei.

The basic ansatz of the RMF theory starts from a Lagrangian density by which nucleons are described as Dirac particles interacting via the exchange of various mesons and the photons. The mesons considered are the scalar sigma (σ), vector omega (ω) and iso-vector vector rho ($\vec{\rho}$). The iso-vector vector rho ($\vec{\rho}$) meson provides the necessary isospin asymmetry. The scalar sigma meson moves in the self-interacting field of cubic and quadratic terms with strengths g_2 and g_3 , respectively. The Lagrangian then consists of the free baryon and meson parts and the interaction part with minimal coupling, together with the nucleon mass M , and $m_\sigma, g_\sigma, m_\omega, g_\omega, m_\rho, g_\rho$ the masses and coupling constants of the respective mesons:

$$\begin{aligned}
\mathcal{L} = & \bar{\psi}(i\rlap{/}\partial - M)\psi + \frac{1}{2}\partial_\mu\sigma\partial^\mu\sigma - U(\sigma) - \frac{1}{4}\Omega_{\mu\nu}\Omega^{\mu\nu} \\
& + \frac{1}{2}m_\omega^2\omega_\mu\omega^\mu - \frac{1}{4}\vec{R}_{\mu\nu}\vec{R}^{\mu\nu} + \frac{1}{2}m_\rho^2\vec{\rho}_\mu\vec{\rho}^\mu - \frac{1}{4}F_{\mu\nu}F^{\mu\nu} \\
& - g_\sigma\bar{\psi}\sigma\psi - g_\omega\bar{\psi}\psi - g_\rho\bar{\psi}\vec{\rho}\vec{\tau}\psi - e\bar{\psi}A\psi.
\end{aligned} \tag{1}$$

The field tensors for the vector mesons are given as:

$$\begin{cases} \Omega^{\mu\nu} = \partial^\mu \omega^\nu - \partial^\nu \omega^\mu, \\ \vec{R}^{\mu\nu} = \partial^\mu \vec{\rho}^\nu - \partial^\nu \vec{\rho}^\mu - g^\rho (\vec{\rho}^\mu \times \vec{\rho}^\nu), \\ F^{\mu\nu} = \partial^\mu \vec{A}^\nu - \partial^\nu \vec{A}^\mu. \end{cases} \quad (2)$$

For a realistic description of nuclear properties, a nonlinear self-coupling of the scalar mesons turns out to be crucial²⁴:

$$U(\sigma) = \frac{1}{2}m_\sigma^2\sigma^2 + \frac{g_2}{3}\sigma^3 + \frac{g_3}{4}\sigma^4 \quad (3)$$

The classical variation principle gives the following equations of motion :

$$[\vec{\alpha} \cdot \vec{p} + V_V(\vec{r}) + \beta(M + V_S(\vec{r}))]\psi_i = \epsilon_i\psi_i \quad (4)$$

for the nucleon spinors and

$$\begin{cases} (-\Delta\sigma + U'(\sigma)) = -g_\sigma\rho_s \\ (-\Delta + m_\omega^2)\omega^\mu = g_\omega j^\mu(\vec{r}) \\ (-\Delta + m_\rho^2)\vec{\rho}^\mu = g_\rho \vec{j}^\mu(\vec{r}) \\ -\Delta A_0^\mu(\vec{r}) = e j_\rho^\mu(\vec{r}) \end{cases} \quad (5)$$

with $U'(\sigma) = \partial_\sigma U(\sigma)$ and $\Delta = -\partial^\mu \partial_\mu$ for the mesons, where

$$\begin{cases} V_V(\vec{r}) = g_\omega\psi + g_\rho\vec{p}\vec{r} + \frac{1}{2}e(1 - \tau_3)\vec{A}, \\ V_S(\vec{r}) = g_\sigma\sigma(\vec{r}) \end{cases} \quad (6)$$

are the vector and scalar potentials respectively and the source terms for the mesons are

$$\begin{cases} \rho_s = \sum_{i=1}^A \bar{\psi}_i \psi_i \\ j^\mu(\vec{r}) = \sum_{i=1}^A \bar{\psi}_i \gamma^\mu \psi_i \\ \vec{j}^\mu(\vec{r}) = \sum_{i=1}^A \bar{\psi}_i \gamma^\mu \vec{\tau} \psi_i \\ j_\rho^\mu(\vec{r}) = \sum_{i=1}^A \bar{\psi}_i \gamma^\mu \frac{1 - \tau_3}{2} \psi_i, \end{cases} \quad (7)$$

where the summations are over the valence nucleons only. It should be noted that as usual, the present approach neglects the contribution of negative energy states, i.e., no-sea approximation, which means that the vacuum is not polarized. The coupled equations

Eq.(4) and Eq.(5) are nonlinear quantum field equations, and their exact solutions are very complicated. Thus the mean field approximation is generally used: i.e., the meson field operators in Eq.(4) are replaced by their expectation values, so that the nucleons move independently in the classical meson fields. The coupled equations are self-consistently solved by iteration.

For spherical nuclei, i.e., the systems with rotational symmetry, the potential of the nucleon and the sources of meson fields depend only on the radial coordinate r . The spinor is characterized by the quantum numbers l, j, m , and the isospin $t = \pm \frac{1}{2}$ for neutron and proton, respectively. The other quantum number is denoted by i . The Dirac spinor has the form:

$$\psi(\vec{r}) = \begin{pmatrix} g \\ f \end{pmatrix} = \begin{pmatrix} i \frac{G_i^{lj}(r)}{r} Y_{jm}^l(\theta, \phi) \\ \frac{F_i^{lj}(r)}{r} (\vec{\sigma} \cdot \hat{r}) Y_{jm}^l(\theta, \phi) \end{pmatrix} \chi_t(t), \quad (8)$$

where $Y_{jm}^l(\theta, \phi)$ are the spinor spherical harmonics and $G_i^{lj}(r)$ and $F_i^{lj}(r)$ are the radial wave function for upper and lower components. They are normalized according to the relation:

$$\int_0^\infty dr (|G_i^{lj}(r)|^2 + |F_i^{lj}(r)|^2) = 1. \quad (9)$$

The radial equation of spinor Eq. (4) can be reduced as :

$$\begin{cases} \epsilon_i G_i^{lj}(r) = \left(-\frac{\partial}{\partial r} + \frac{\kappa_i}{r}\right) F_i^{lj}(r) + (M + V_S(r) + V_V(r)) G_i^{lj}(r) \\ \epsilon_i F_i^{lj}(r) = \left(+\frac{\partial}{\partial r} + \frac{\kappa_i}{r}\right) G_i^{lj}(r) - (M + V_S(r) - V_V(r)) F_i^{lj}(r), \end{cases} \quad (10)$$

where

$$\kappa = \begin{cases} -(j + 1/2) & \text{for } j = l + 1/2 \\ +(j + 1/2) & \text{for } j = l - 1/2. \end{cases}$$

The meson field equations become simply radial Laplace equations of the form:

$$\left(-\frac{\partial^2}{\partial r^2} - \frac{2}{r} \frac{\partial}{\partial r} + m_\phi^2\right) \phi = s_\phi(r), \quad (11)$$

m_ϕ are the meson masses for $\phi = \sigma, \omega, \rho$ and for photon ($m_\phi = 0$). The source terms are:

$$s_\phi(r) = \begin{cases} -g_\sigma \rho_s - g_2 \sigma^2(r) - g_3 \sigma^3(r) & \text{for the } \sigma \text{ field} \\ g_\omega \rho_v & \text{for the } \omega \text{ field} \\ g_\rho \rho_3(r) & \text{for the } \rho \text{ field} \\ e \rho_c(r) & \text{for the Coulomb field,} \end{cases} \quad (12)$$

$$\begin{cases} 4\pi r^2 \rho_s(r) = \sum_{i=1}^A (|G_i(r)|^2 - |F_i(r)|^2) \\ 4\pi r^2 \rho_v(r) = \sum_{i=1}^A (|G_i(r)|^2 + |F_i(r)|^2) \\ 4\pi r^2 \rho_3(r) = \sum_{p=1}^Z (|G_p(r)|^2 + |F_p(r)|^2) - \sum_{n=1}^N (|G_n(r)|^2 + |F_n(r)|^2) \\ 4\pi r^2 \rho_c(r) = \sum_{p=1}^Z (|G_p(r)|^2 + |F_p(r)|^2). \end{cases} \quad (13)$$

The Laplace equation can be solved by using the Green function:

$$\phi(r) = \int_0^\infty r'^2 dr' G_\phi(r, r') s_\phi(r'), \quad (14)$$

where for massive fields

$$G_\phi(r, r') = \frac{1}{2m_\phi} \frac{1}{rr'} (e^{-m_\phi|r-r'|} - e^{-m_\phi|r+r'|}) \quad (15)$$

and for Coulomb field

$$G_\phi(r, r') = \begin{cases} 1/r & \text{for } r > r' \\ 1/r' & \text{for } r < r'. \end{cases} \quad (16)$$

The Eqs.(10) and (11) could be solved self-consistently in the usual RMF approximation. However, Eq.(10) does not contain the pairing interaction, as the classical meson fields are used in RMF. In order to have the pairing interaction, one has to quantize the meson fields which leads to a Hamiltonian with two-body interaction. Following the standard procedure of Bogoliubov transformation, a Dirac Hartree-Bogoliubov equation could be derived and then a unified description of the mean field and pairing correlation in nuclei could be achieved. For the details, see Ref.² and the references therein. The RHB equations are as following:

$$\int d^3r' \begin{pmatrix} h - \lambda & \Delta \\ \Delta & -h + \lambda \end{pmatrix} \begin{pmatrix} \psi_U \\ \psi_V \end{pmatrix} = E \begin{pmatrix} \psi_U \\ \psi_V \end{pmatrix}, \quad (17)$$

where

$$h(\vec{r}, \vec{r}') = [\vec{\alpha} \cdot \vec{p} + V_V(\vec{r}) + \beta(M + V_S(\vec{r}))] \delta(\vec{r}, \vec{r}') \quad (18)$$

is the Dirac Hamiltonian and the Fock term has been neglected as is usually done in RMF.

The pairing potential is :

$$\Delta_{kk'}(\vec{r}, \vec{r}') = - \int d^3r_1 \int d^3r'_1 \sum_{\tilde{k}\tilde{k}'} V_{kk', \tilde{k}\tilde{k}'}(\vec{r}\vec{r}'; \vec{r}_1\vec{r}'_1) \kappa_{\tilde{k}\tilde{k}'}(\vec{r}_1, \vec{r}'_1). \quad (19)$$

It is obtained from the one-meson exchange interaction $V_{kk', \tilde{k}\tilde{k}'}(\vec{r}\vec{r}'; \vec{r}_1\vec{r}'_1)$ in the pp -channel and the pairing tensor $\kappa = V^*U^T$:

$$\kappa_{kk'}(\vec{r}, \vec{r}') = \langle |a_k a_{k'}| \rangle = \psi_V^k(\vec{r})^* \psi_U^{k'}(\vec{r})^T. \quad (20)$$

The nuclear density is as following:

$$\rho(\vec{r}, \vec{r}') = \sum_{ilj} g_{ilj} \psi_V^{ilj}(\vec{r})^* \psi_V^{ilj}(\vec{r}'). \quad (21)$$

As in Ref.², V used for the pairing potential in Eq.(19) is either the density-dependent two-body force of zero range with the interaction strength V_0 and the nuclear matter density ρ_0 :

$$V(\mathbf{r}_1, \mathbf{r}_2) = V_0 \delta(\mathbf{r}_1 - \mathbf{r}_2) \frac{1}{4} [1 - \boldsymbol{\sigma}_1 \boldsymbol{\sigma}_2] \left(1 - \frac{\rho(r)}{\rho_0} \right), \quad (22)$$

or Gogny-type finite range force with the parameter μ_i , W_i , B_i , H_i and M_i ($i = 1, 2$):²⁵

$$V(\mathbf{r}_1, \mathbf{r}_2) = \sum_{i=1,2} e^{((\mathbf{r}_1 - \mathbf{r}_2)/\mu_i)^2} (W_i + B_i P^\sigma - H_i P^\tau - M_i P^\sigma P^\tau). \quad (23)$$

A Lagrange multiplier λ is introduced to fix the particle number for the neutron and proton as $N = \text{Tr} \rho_n$ and $Z = \text{Tr} \rho_p$.

In order to describe both continuum and bound states self-consistently, we use the RHB theory in coordinate representation, i.e., the Relativistic Continuum Hartree-Bogolyubov (RCHB) theory². It is then applicable to both exotic nuclei and normal nuclei. In Eq. (17), the eigenstates occur in pairs of opposite energies. When spherical symmetry is imposed on the solution of the RCHB equations, the wave function can be written as:

$$\psi_U^i = \left(\begin{array}{c} i \frac{G_U^{ij}(r)}{r} \\ \frac{F_U^{ij}(r)}{r} (\vec{\sigma} \cdot \hat{r}) \end{array} \right) Y_{jm}^l(\theta, \phi) \chi_t(t), \psi_V^i = \left(\begin{array}{c} i \frac{G_V^{ij}(r)}{r} \\ \frac{F_V^{ij}(r)}{r} (\vec{\sigma} \cdot \hat{r}) \end{array} \right) Y_{jm}^l(\theta, \phi) \chi_t(t). \quad (24)$$

Using the above equation, Eq.(17) depends only on the radial coordinates and can be expressed as the following integro-differential equation:

$$\left\{ \begin{array}{l} \frac{dG_U(r)}{dr} + \frac{\kappa}{r} G_U(r) - (E + \lambda - V_V(r) + V_S(r)) F_U(r) + r \int r' dr' \Delta(r, r') F_V(r') = 0 \\ \frac{dF_U(r)}{dr} - \frac{\kappa}{r} F_U(r) + (E + \lambda - V_V(r) - V_S(r)) G_U(r) + r \int r' dr' \Delta(r, r') G_V(r') = 0 \\ \frac{dG_V(r)}{dr} + \frac{\kappa}{r} G_V(r) + (E - \lambda + V_V(r) - V_S(r)) F_V(r) + r \int r' dr' \Delta(r, r') F_U(r') = 0 \\ \frac{dF_V(r)}{dr} - \frac{\kappa}{r} F_V(r) - (E - \lambda + V_V(r) + V_S(r)) G_V(r) + r \int r' dr' \Delta(r, r') G_U(r') = 0, \end{array} \right. \quad (25)$$

where the nucleon mass is included in the scalar potential $V_S(r)$. For the δ -force of Eq.(22), Eq.(25) is reduced to normal coupled differential equations and can be solved with shooting method by Runge-Kutta algorithms. For the case of Gogny force, the coupled integro-differential equations are discretized in the space and solved by the finite element methods. The numerical details can be found in Ref.². Now we have to solve Eqs.(25) and (11) self-consistently for the RCHB case. As the calculation with Gogny force is very time-consuming, we solve them only for one case in order to fix the interaction strength for δ -force in Eq.(22).

3. The pseudo-spin symmetry

The Dirac equation in RMF or in the canonical basis of RCHB describes a Dirac spinor with mass M moving in a scalar potential $V_S(\vec{r})$ and a vector potential $V_V(\vec{r})$. With $\epsilon = M + E$, the potential $V = V_V(\vec{r}) + V_S(\vec{r})$, which is around -50 MeV, and the effective mass $M^* = M + V_S(\vec{r})$, the relation between the upper and lower components of the wave function can be written as:

$$\left\{ \begin{array}{l} g = \frac{1}{E - V} (\vec{\sigma} \cdot \vec{p}) f \\ f = \frac{1}{E + 2M^* - V} (\vec{\sigma} \cdot \vec{p}) g \end{array} \right. \quad (26)$$

Then the coupled equations are reduced to uncoupled ones for the upper and lower components, respectively. Effectively we get the corresponding Schrödinger equation for both components:

$$\begin{cases} (\vec{\sigma} \cdot \vec{p}) \frac{1}{E + 2M^* - V} (\vec{\sigma} \cdot \vec{p}) g = (E - V) g \\ (\vec{\sigma} \cdot \vec{p}) \frac{1}{E - V} (\vec{\sigma} \cdot \vec{p}) f = (E + 2M^* - V) f \end{cases} \quad (27)$$

In the spherical case, V depends only on the radius. We choose the phase convention of the vector spherical harmonics as:

$$(\vec{\sigma} \cdot \vec{r}) Y_{jm}^l = -Y_{jm}^{l'} \quad (28)$$

where

$$l' = 2j - l = \begin{cases} l + 1, & j = l + 1/2 \\ l - 1, & j = l - 1/2 \end{cases} \quad (29)$$

Here l' is nothing but the pseudo-orbital angular momentum \tilde{l} . After some tedious procedures, one gets the radial equation for the lower and upper components respectively:

$$\begin{aligned} & \left[\frac{d^2}{dr^2} + \frac{1}{E - V} \frac{dV}{dr} \frac{d}{dr} \right] F_i^{lj}(r) \\ & + \left[\frac{\kappa(1 - \kappa)}{r^2} - \frac{1}{E - V} \frac{\kappa}{r} \frac{dV}{dr} \right] F_i^{lj}(r) \\ = & - (E + 2M^* - V)(E - V) F_i^{lj}(r), \end{aligned} \quad (30)$$

$$\begin{aligned} & \left[\frac{d^2}{dr^2} - \frac{1}{E + 2M^* - V} \frac{d(2M^* - V)}{dr} \frac{d}{dr} \right] G_i^{lj}(r) \\ & - \left[\frac{\kappa(1 + \kappa)}{r^2} + \frac{1}{E + 2M^* - V} \frac{\kappa}{r} \frac{d(2M^* - V)}{dr} \right] G_i^{lj}(r) \\ = & - (E + 2M^* - V)(E - V) G_i^{lj}(r), \end{aligned} \quad (31)$$

where

$$\kappa(\kappa - 1) = l'(l' + 1), \quad \kappa(\kappa + 1) = l(l + 1). \quad (32)$$

It is clear that one can use either Eq.(30) or equivalently Eq.(31) to get the eigenvalues E and the corresponding eigenfunctions. Normally Eq.(31) is used in the literature and the

spin-orbital splitting is discussed in connection with the corresponding spin-orbital potential $\frac{1}{E + 2M^* - V} \frac{\kappa}{r} \frac{d(2M^* - V)}{dr}$. If the Eq. (30) is used instead and the pseudo spin-orbital potential (PSOP) term, $\frac{1}{E - V} \frac{\kappa}{r} \frac{dV}{dr}$, is neglected, then the eigenvalues E for the same l' will degenerate. This is the phenomenon of pseudo-spin symmetry observed in^{3,4}. It means that Eq.(26) is the transformation between the normal spin formalism and the pseudo-spin formalism.

In Eq. (30), the term which splits the pseudo-spin partners is simply the PSOP. The hidden symmetry for the pseudo-spin approximation is revealed as $dV/dr = 0$, which is more general and includes $V = 0$ discussed in¹⁶ as a special case. For exotic nuclei with highly diffuse potentials, $dV/dr \sim 0$ may be a good approximation and then the pseudo-spin symmetry will be good. But generally, $dV/dr = 0$ is not always satisfied in the nuclei and the pseudo-spin symmetry is an approximation. However, if $|\frac{1}{E - V} \frac{\kappa}{r} \frac{dV}{dr}| \ll |\frac{\kappa(1 - \kappa)}{r^2}|$, the pseudo-spin approximation will be good. Thus, the comparison of the relative magnitude of the centrifugal barrier (CB), $\frac{\kappa(1 - \kappa)}{r^2}$, and the PSOP can provide us with some information on the pseudo-spin symmetry.

In a recent letter¹, the mechanism behind the pseudo-spin symmetry was studied and the pseudo-spin symmetry was shown to be connected with the competition between the centrifugal barrier (CB) and the pseudo-spin orbital potential (PSOP), which is mainly decided by the derivative of the difference between the scalar and vector potentials. With the scalar and vector potentials derived from a self-consistent RCHB calculation, the pseudo-spin symmetry and its energy dependence have been discussed. Here in this paper we will extend the previous investigation to the case of exotic nuclei. The pseudo-spin symmetry for exotic nuclei is investigated for Zr and Sn isotopes from the proton drip line to the neutron drip line. The isospin and energy dependence of the pseudo-spin approximation will be investigated in detail in the following section.

4. The energy splitting of the pseudo-spin partners

We use here the non-linear Lagrangian parameter set NLSH²⁶ which could provide a good description of all nuclei from oxygen to lead. As we study not only the closed shell nuclei, but also the open shell nuclei, the inclusion of the pairing is necessary. The pairing interaction strength is the same as in Ref.²². The interaction strength in the pairing force of zero range Eq.(22) is properly renormalized by the calculation of RCHB with Gogny force. Since we use a pairing force of zero range, we have to limit the number of continuum levels by a cut-off energy. For each spin-parity channel, 20 radial wave functions are taken into account, which corresponds roughly to a cut-off energy of 120 MeV for a fixed box radius $R = 20$ fm. For the fixed cut-off energy and for the box radius R , the strength V_0 of the pairing force in Eq.(22) is determined by adjusting the corresponding pairing energy $-\frac{1}{2}\text{Tr}\Delta\kappa$ to that of a RCHB-calculation using the finite range part of the Gogny force D1S²⁵. We use the nuclear matter density 0.152 fm^{-3} for ρ_0 .

The quality of pseudo-spin symmetry can be understood more clearly by considering the microscopic structure of the wave functions and the single particle energies in the canonical basis. As shown in Ref.², the particle levels for the bound states in canonical basis are the same as those by solving the Dirac equation with the scalar and vector potentials from RCHB. Therefore Eqs. (30) and (31) are valid in canonical basis after the pairing interaction has been taken into account and are very suitable for the discussion of the pseudo-spin symmetry.

The neutron single particle levels in ¹⁵⁰Sn and ¹²⁰Zr are given in Fig. 1a and 1b, respectively. The four sets of pseudo-spin partners, i.e., $1d_{3/2}$ and $2s_{1/2}$, $1f_{5/2}$ and $2p_{3/2}$, $1g_{7/2}$ and $2d_{5/2}$, $2d_{3/2}$ and $3s_{1/2}$, are marked by boxes. As seen in the figure, the energy splitting between pseudo-spin partners decreases with the decreasing binding energy. The single particle energy of $3s_{1/2}$ in ¹²⁰Zr is -6.00 MeV, and its partner $2d_{3/2}$ is -5.86 MeV, the splitting is 0.14 MeV. While $2s_{1/2}$ is -31.62 MeV, $1d_{3/2}$ -33.23 MeV, the splitting is 1.61 MeV, which is bigger than the former one by a factor of 10. The same situation is found

for the energy splitting between pseudo-spin partners in ^{150}Sn : The single particle energies of $3s_{1/2}$ and $2d_{3/2}$ are -9.645 and -10.11 MeV, respectively. The single particle energies for other pseudo-spin partners in ^{150}Sn are, -11.74 and -13.87 MeV for $2d_{5/2}$ and $1g_{7/2}$ partners, -22.46 and -25.50 MeV for $2p_{3/2}$ and $1f_{5/2}$ partners, -33.63 and -36.58 for $2s_{1/2}$ and $1d_{3/2}$ partners, respectively. Although we show only the neutron single particle levels in ^{150}Sn and ^{120}Zr as examples here, the same are found in other Sn and Zr isotopes. It is usually seen that the pseudo-spin symmetry approximation becomes better near the Fermi surface, which is in agreement with the experimental observation.

In Fig.1 there are also two pairs of pseudo-spin partners ($3p_{3/2}$ and $2f_{5/2}$ partners and $2f_{7/2}$ and $1h_{9/2}$ partners) near the threshold, apart from the four pairs of pseudo-spin partners below the Fermi level. The energies for these two pairs of pseudo-spin partners are -1.581 and -1.031 MeV for the $3p_{3/2}$ and $2f_{5/2}$ partners, and -2.549 and -2.620 MeV for the $2f_{7/2}$ and $1h_{9/2}$ partners, respectively. Considering their pseudo-spin orbital angular momentum $\tilde{l} = 2$ and 4 , their splittings $\Delta E = \frac{E_{\tilde{l}j=\tilde{l}-1/2} - E_{\tilde{l}j=\tilde{l}+1/2}}{2\tilde{l} + 1}$ are only -0.1100 MeV and 0.7889×10^{-2} MeV, respectively. This is due to the energy dependence and the diffuseness of the potential in exotic nuclei, which we will discuss in the following. As it is seen in Fig.1, the normal splitting is such that the orbital $j = \tilde{l} + 1/2$ is below the orbital $j = \tilde{l} - 1/2$, except for $3p_{3/2}$ and $2f_{5/2}$ partners. The same also happens for $2d_{3/2}$ and $3s_{1/2}$ partners in Zr isotopes. The pseudo-spin splitting depends on the derivative of the difference between the scalar and vector potentials dV/dr , which is small for the exotic nuclei with highly diffuse potential. The integration of $\frac{dV}{dr}|F|^2$ over r gives the splitting of the pseudo-spin partners, whose sign will decide the normal splitting or the reverse. The subtle details of the potential are crucial for the pseudo-spin splitting.

To see the behavior of the pseudo-spin partners around the Fermi level and the isospin dependence of the pseudo-spin splitting, we show the single particle levels near the Fermi surface in the canonical basis for the Sn and Zr isotopes with an even neutron number as a function of the mass number in Fig. 2. The Fermi level is shown by the dashed line. The pseudo-spin splitting for the pseudo-spin partners, $2d_{3/2}$ and $3s_{1/2}$, remains small in

Zr and Sn isotopes from the proton drip line to the neutron drip line. The pseudo-spin symmetry remains even valid for exotic nuclei. The pseudo-spin symmetry near the neutron drip line becomes better than that near the β -stability line. In Fig. 2a, there is a kink for the single particle levels in the continuum, as the contribution from the continuum becomes important and the potential becomes diffuse around ^{130}Sn . But the splitting for $3p_{3/2}$ and $2f_{5/2}$ partners, and $2f_{7/2}$ and $1h_{9/2}$ partners in Sn isotopes is small and the pseudo-spin symmetry approximation is very good, independent of whether they are in the continuum or near the threshold. Therefore we can see that the pseudo-spin symmetry is very well reserved for the orbital near the threshold energy and in the continuum region.

In order to see the energy dependence and the isospin dependence of the pseudo-spin orbital splitting more clearly, we plot $\Delta E = \frac{E_{\tilde{l}j=\tilde{l}-1/2} - E_{\tilde{l}j=\tilde{l}+1/2}}{2\tilde{l}+1}$ versus $E = \frac{\tilde{l}E_{\tilde{l}j=\tilde{l}+1/2} + (\tilde{l}+1)E_{\tilde{l}j=\tilde{l}-1/2}}{2\tilde{l}+1}$ for the bound pseudo-spin partners in Sn and Zr isotopes in Fig. 3. In both isotopes, a monotonous decreasing behavior with the decreasing binding energy is clearly seen. The pseudo-spin splitting for $3s_{1/2}$ and $2d_{3/2}$ is more than 10 times smaller than that of the $2s_{1/2}$ and $1d_{3/2}$. As far as the isospin dependence of the pseudo-spin orbital splitting is concerned, the splitting in Sn isotopes gives a monotonous decreasing behavior with the increasing isospin. Particularly for $2s_{1/2}$ and $1d_{3/2}$ partners, the pseudo-spin splitting in ^{170}Sn is only half of that in ^{96}Sn . Just as we expected, the pseudo-spin symmetry in neutron-rich nuclei is better. In Zr isotopes, although the situation is more complicated (e.g., the effect of the deformation which is neglected here), the pattern is more or less the same, i.e., a monotonous decreasing behavior with the decreasing binding energy and a monotonous decreasing behavior with the isospin. From these studies, we see that the pseudo-spin symmetry remains a good approximation for both stable and exotic nuclei. A better pseudo-spin symmetry can be expected for the orbital near the threshold, particularly for nuclei near the particle drip-line.

5. The pseudo-spin orbital potential

To understand why the energy splitting of the pseudo-spin partner changes with different binding energies and why the pseudo-spin approximation is good in RMF, the PSOP and CB should be examined carefully. Unfortunately, it is very hard to compare them clearly, as the PSOP has a singularity at $E \sim V$. As we are only interested in the relative magnitude of the CB and the PSOP, we introduce the effective CB, $(E - V)\frac{\kappa(\kappa - 1)}{r^2}$, and the effective PSOP, $\frac{\kappa}{r}\frac{dV}{dr}$, for comparison. They correspond to the CB and the PSOP multiplied by a common factor $E - V$ respectively.

The effective PSOP does not depend on the binding energy of the single particle level, but depends on the angular momentum and parity. On the other hand the effective CB depends on the energy. Comparing these two effective potentials one could see the energy dependence of the pseudo-spin symmetry. They are given in Fig. 4 for $s_{1/2}$ (lower) and $d_{3/2}$ (upper) of ^{120}Zr in arbitrary scale.

The pseudo-spin approximation is much better for the less bound pseudo-spin partners, because the effective CB is smaller for the more deeply bound states. This is in agreement with the results shown in Fig.3. The effective PSOP and the effective CB are also given as inserts in Fig.4 in order to show their behavior near the nuclear surface.

In order to examine this carefully, we compare the effective CB (dashed lines or dot-dashed lines) and the effective PSOP (solid lines) multiplied by the squares of the lower component wave function $F(r)$, which are given in Fig. 5, for $2s_{1/2}$ (upper left), $3s_{1/2}$ (lower left), $1d_{3/2}$ (upper right), and $2d_{3/2}$ (lower right) of ^{120}Zr in arbitrary scale. The pseudo-spin approximation is much better for the less bound pseudo-spin partners, because the effective CB is smaller for the more deeply bound states. This is in agreement with the results shown above. The integrated values of the potentials in Fig.2 with r are proportional to their contribution to the energy after some proper renormalization. It is clear that the contribution of the effective CB (dashed lines or dot-dashed lines) is much bigger than that of the effective PSOP (solid lines). Generally the effective PSOP is two orders of

magnitude smaller than the effective CB.

In Fig. 1 and 2 we notice that the orbital $j = \tilde{l} + 1/2$ is generally below the orbital $j = \tilde{l} - 1/2$, except for $3p_{3/2}$ and $2f_{5/2}$ partners in Sn isotopes. The same situation also happens for $2d_{3/2}$ and $3s_{1/2}$ partners in Zr isotopes. As the pseudo-spin splitting depends on PSOP, which depends on the subtle radial dependence of the potentials, sometimes the PSOP may have positive or negative regions as a function of r which cancel each other. The integration of $\frac{dV}{dr}|F|^2$ over r gives the splitting of the pseudo-spin partners, whose sign will decide the normal splitting or the reverse. That is the reason why the orbital $j = \tilde{l} + 1/2$ is above the orbital $j = \tilde{l} - 1/2$ for $3p_{3/2}$ and $2f_{5/2}$ partners in Sn isotopes and for $2d_{3/2}$ and $3s_{1/2}$ partners in Zr isotopes.

6. The wave-function of pseudo-spin partners

In the above discussion, we have seen that the PSOP is much smaller than the CB. Therefore if we neglect the PSOP in Eq.(30), the lower component of the Dirac wave functions for the pseudo-spin partners will be the same, i.e., in the case of the exact pseudo-spin symmetry, the lower component of the pseudo-spin partners should be identical (except for the phase). The upper component of the Dirac wave functions can be obtained from the transformation in Eq.(26), which depends on the quantum number κ . Therefore the study of the Dirac wave functions for the pseudo-spin partners will provide a check for the pseudo-spin approximation in nuclei. As examples, the normalized single nucleon wave functions for the upper (G) and lower (F) components of the Dirac wave functions for the pseudo-spin partners $1d_{3/2}$ and $2s_{1/2}$, $1f_{5/2}$ and $2p_{3/2}$, $1g_{7/2}$ and $2d_{5/2}$, $2d_{3/2}$ and $3s_{1/2}$ in ^{120}Zr are given in Fig. 6. Of course, the lower components are much smaller in magnitude compared with the upper component in Eq.(26). The phase of the Dirac wave functions for one of the pseudo-spin partners has been reversed in order to have a careful comparison. It is seen that the lower components of the Dirac wave functions for the pseudo-spin partners are very similar and are almost equal in magnitude, as observed also for ^{208}Pb in Ref.¹⁸. The similarity in the lower components

F of the wave function for the pseudo-spin partners near the Fermi surface is better than for the deeply bound ones. The lower components for the pseudo-spin partners with small pseudo-spin orbital angular momentum are better than for the ones with large pseudo-spin orbital angular momentum. As seen in Fig.6, the similarity for pseudo-spin partners $2d_{3/2}$ and $3s_{1/2}$ is better than for pseudo-spin partners $1d_{3/2}$ and $2s_{1/2}$. The similarities for pseudo-spin partners, $2d_{3/2}$ and $3s_{1/2}$, $1d_{3/2}$ and $2s_{1/2}$, are better than for the pseudo-spin partners $1f_{5/2}$ and $2p_{3/2}$, $1g_{7/2}$ and $2d_{5/2}$.

Although the lower components for the pseudo-spin partners are very close to each other, the difference for the upper components is very big. The upper component of the Dirac wave functions can be obtained from the transformation in Eq.(26), which for the spherical case can be reduced to the follows:

$$G_i^{lj}(r) = \frac{1}{E - V} \left[-\frac{dF_i^{lj}(r)}{dr} + \frac{\kappa}{r} F_i^{lj}(r) \right]. \quad (33)$$

As seen in Fig.6, in the case of exact pseudo-spin symmetry, where both E and $F_i^{lj}(r)$ are identical for the pseudo-spin partners, the upper components $G_i^{lj}(r)$ will be different due to the term $\frac{\kappa}{r} F_i^{lj}(r)$. For the pseudo-spin partners with small \tilde{l} , the contribution of the term $\frac{\kappa}{r} F_i^{lj}(r)$ becomes less important for larger r and a similarity between the upper components can happen in the nuclear surface. As for examples, for $r \geq 6$ fm, the upper components for the pseudo-spin partners $1d_{3/2}$ and $2s_{1/2}$, $1f_{5/2}$ and $2p_{3/2}$, $2d_{3/2}$ and $3s_{1/2}$, in Fig. 6 are very similar.

7. Summary

In conclusion, the pseudo-spin symmetry is examined in normal and exotic nuclei in the framework of RCHB theory. Based on RCHB theory the pseudo-spin approximation in exotic nuclei is investigated in Zr and Sn isotopes from the proton drip line to the neutron drip line. The quality of the pseudo-spin approximation is shown to be connected with the competition between the centrifugal barrier (CB) and the pseudo-spin orbital potential (PSOP), which is mainly decided by the derivative of the difference between the scalar and vector potentials

dV/dr . If the derivative of the difference between the scalar and vector potentials dV/dr vanishes, the pseudo-spin symmetry is exact. The condition $dV/dr \sim 0$ may be a good approximation for the exotic nuclei with highly diffuse potential. Further the new condition $\frac{1}{E-V} \frac{\kappa dV}{r dr} \ll \frac{\kappa(1-\kappa)}{r^2}$ is found under which the symmetry is preserved approximately. We have examined this condition to see how good the pseudo-spin symmetry is in RCHB. For a given angular momentum and parity channel, the effective CB, $(E-V) \frac{\kappa(\kappa-1)}{r^2}$, becomes stronger for the less bound level, so the pseudo-spin symmetry for the weakly bound state is better than that for the deeply bound state, which is in agreement with the experimental observation^{3,4}. The pseudo-spin symmetry is found to be a good approximation even for the exotic nuclei with highly diffuse potential. The above conclusion has been well supported by RCHB calculations for Zr and Sn isotopes from the proton drip line to the neutron drip line. From the simple Dirac equation, it has been shown that there are two equivalent ways to solve the coupled Dirac equation for the upper and lower components: i.e., the normal spin formalism and pseudo-spin formalism. Both formalisms are equivalent as far as the energies and wave functions are concerned. Their relation is given by Eq.(26), which indicates that the unitary transformation from the conventional formalism to the pseudo-spin formalism has the "p-helicity"^{14,11,17}. Summarizing our investigation, we conclude:

- 1 The quality of the pseudo-spin approximation is connected with the competition between the CB, and the PSOP which is mainly proportional to the derivative of the difference between the scalar and vector potentials dV/dr ;
- 2 The pseudo-spin symmetry is a good approximation for normal nuclei and become much better for exotic nuclei with highly diffuse potentials;
- 3 The pseudo-spin symmetry has strong energy dependence. The energy splitting between the pseudo-spin partners is smaller for orbitals near the Fermi surface.
- 4 The energy difference between the orbital $j = \tilde{l} + 1/2$ and the orbital $j = \tilde{l} - 1/2$ is always negative, except for $3p_{3/2}$ and $2f_{5/2}$ partners. The same situation also happens

for $2d_{3/2}$ and $3s_{1/2}$ partners in Zr isotopes. The integration of $\frac{dV}{dr}|F|^2$ over r gives the splitting of the pseudo-spin partners, whose sign will decide the normal splitting or the reverse.

- 5 The lower components of the Dirac wave functions for the pseudo-spin partners are very similar and almost equal in magnitude. The similarity in the lower components of the wave function for the pseudo-spin partners near the Fermi surface is closer than for the deeply bound ones.

REFERENCES

1. J. Meng, K.Sugawara-Tanabe, S.Yamaji, P. Ring and A.Arima, Phys. Rev. C58 (1998) R628.
2. J.Meng, Nucl.Phys. **A 635** (1998) 3.
3. A.Arima, M.Harvey and K.Shimizu, Phys.Lett.B30 (1969) 517.
4. K.T.Hecht and A.Adler, Nucl.Phys.**A 137** (1969) 129.
5. R.D.Ratna Raju, J. P. Draayer and K.T.Hecht, Nucl.Phys. **A 202** (1973) 433; J. P. Draayer and K. J. Weeks, Ann. Phys. (N.Y.) 156 (1984) 41.
6. A.L. Blokhin, T.Beuschel, J. P. Draayer and C. Bahri, Nucl. Phys. **A612** (1997) 163. T.Beuschel, A.L. Blokhin and J. P. Draayer, Nucl. Phys. **A619** (1997) 119.
7. B. Mottelson, Nucl. Phys. **A522**, 1 (1991).
8. J.Y. Zeng, J. Meng, C. S. Wu, E. G. Zhao, Z. Xing and X. Q. Chen, Phys. Rev. C **44** (1991) R1745.
9. C. Bahri, J. P. Draayer and S. A. Moszkowski, Phys. Rev. Lett. **68** (1992) 2133.
10. O. Castanos, M. Moshinsky, and C. Quesne, Phys. Letts. **B277** (1992) 238.
11. A. L. Blokhin, C. Bahri, J. P. Draayer, J. Phys. **A29** (1996) 2039.
12. A. Bohr, I. Hamamoto and B. R. Mottelson, Phys. Scripta **26** (1982) 267.
13. A.B. Balantekin, O. Castañov and M. Moshinsky, Phys.Lett. **B284** (1992) 1.
14. A.L.Blokhin, C.Bahri and J.P.Draayer, Phys.Rev.Lett. 74 (1995) 4149.
15. B. D. Serot and J. D. Walecka, *The Relativistic Nuclear Many-Body Problem in Advances in Nuclear Physics*, edited by J. W. Negele and E. Vogt, Vol. **16** (Plenum, New York, 1986).

16. J.Ginocchio, Phys. Rev. Lett. **78** (1997) 436.
17. J.N. Ginocchio, and A. Leviatan, Phys. Lett. **B425** (1998) 1.
18. J.N. Ginocchio, and D. G. Madland, Phys.Rev. C57 (1998) 1167.
19. I.Tanihata, Prog. in Part.and Nucl.Phys.,**35** (1995) 505
20. P.G. Hansen, A.S. Jensen, and B. Jonson, Ann. Rev. Nucl. Part. Sci. **45** (1995) 591
21. J. Meng and P. Ring, Phys. Rev. Lett. **77** (1996) 3963.
22. J. Meng and P. Ring, Phys. Rev. Lett. **80** (1998) 460.
23. J. Meng, I. Tanihata and S. Yamaji, Phys. Lett. **B419** (1998) 1
24. J. Boguta, A.R. Bodmer, Nucl. Phys. **A292** (1977) 413
25. J.F. Berger et al, Nucl. Phys. **A428** (1984) 32c
26. M.Sharma, M.Nagarajan and P.Ring, Phys.Lett. **B312** (1993) 377.

Figure Captions

Fig. 1 The single particle levels in the canonical basis for the neutron in ^{120}Zr and ^{150}Sn .

The Fermi surface is shown by a dashed line. The bound pseudo-spin partners are marked by boxes

Fig. 2 The single particle energies of the neutron in the canonical basis as a function of the mass number for Zr and Sn isotopes. The dashed line indicates the chemical potential.

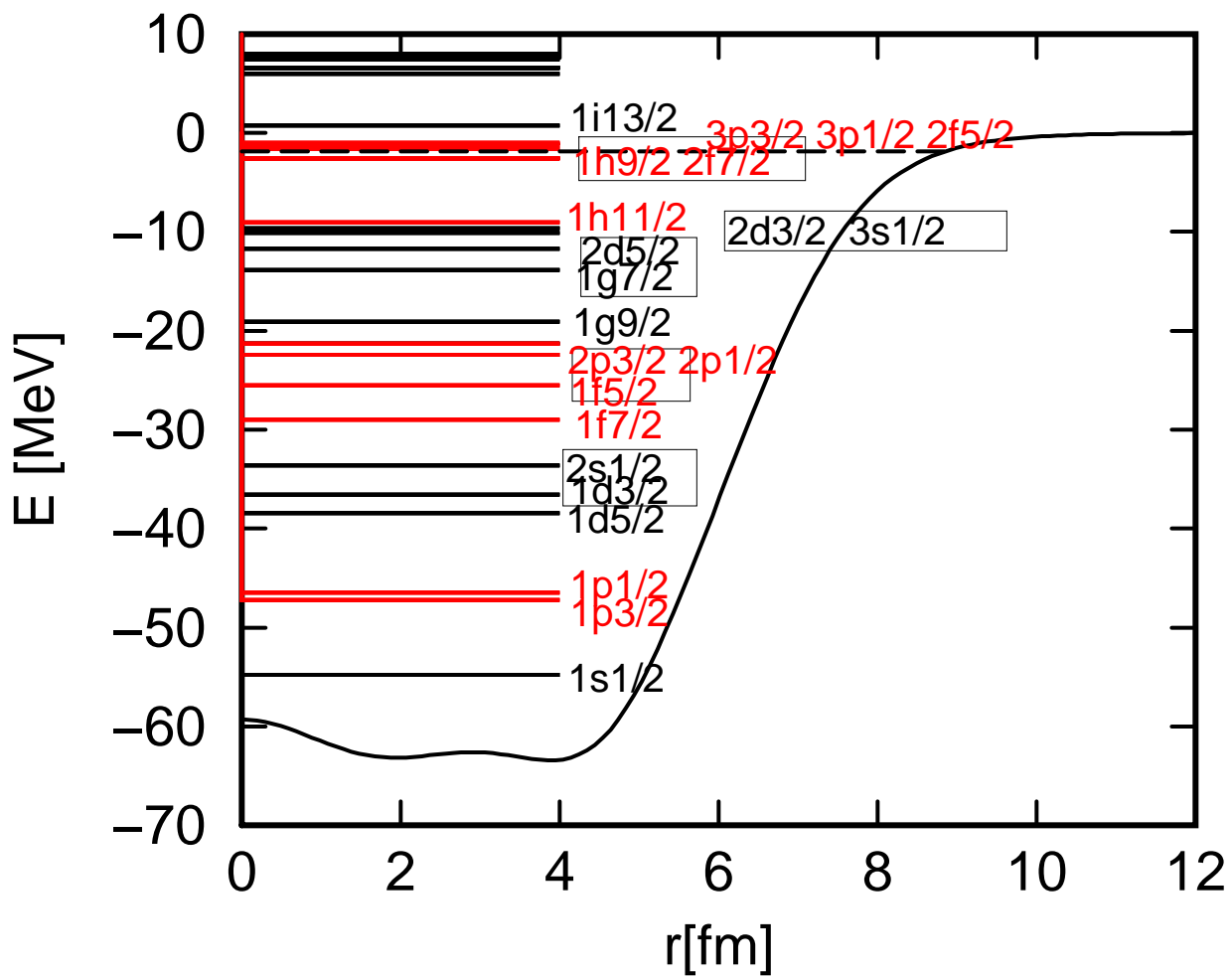
Fig. 3 The pseudo-spin orbit splitting $\Delta E = \frac{E_{\tilde{l}j=\tilde{l}-1/2} - E_{\tilde{l}j=\tilde{l}+1/2}}{2\tilde{l}+1}$ versus the binding energy $E = \frac{\tilde{l}E_{\tilde{l}j=\tilde{l}+1/2} + (\tilde{l}+1)E_{\tilde{l}j=\tilde{l}-1/2}}{2\tilde{l}+1}$ for Zr and Sn isotopes. From left to right, the pseudo-spin partners correspond to $(1d_{3/2}, 2s_{1/2})$, $(1f_{5/2}, 2p_{3/2})$, $(1g_{7/2}, 2d_{5/2})$ and $(2d_{3/2}, 3s_{1/2})$, respectively.

Fig. 4 The comparison of the effective centrifugal barrier (CB) $(E - V)\frac{\kappa(\kappa - 1)}{r^2}$ (dashed lines and dot-dashed lines) and the effective pseudo-spin orbital potential (PSOP) $\frac{\kappa}{r} \frac{dV}{dr}$ (solid line) in arbitrary scale for $d_{3/2}$ (upper) and $s_{1/2}$ (lower) in ^{120}Zr . The dashed lines are for $1d_{3/2}$ and $2s_{1/2}$, and the dot-dashed lines are for $2d_{3/2}$ and $3s_{1/2}$. The inserted boxes show the same quantities, but the ordinate is magnified and the abscissa is reduced to show the behaviors of the effective CB and the effective PSOP near the nuclear surface.

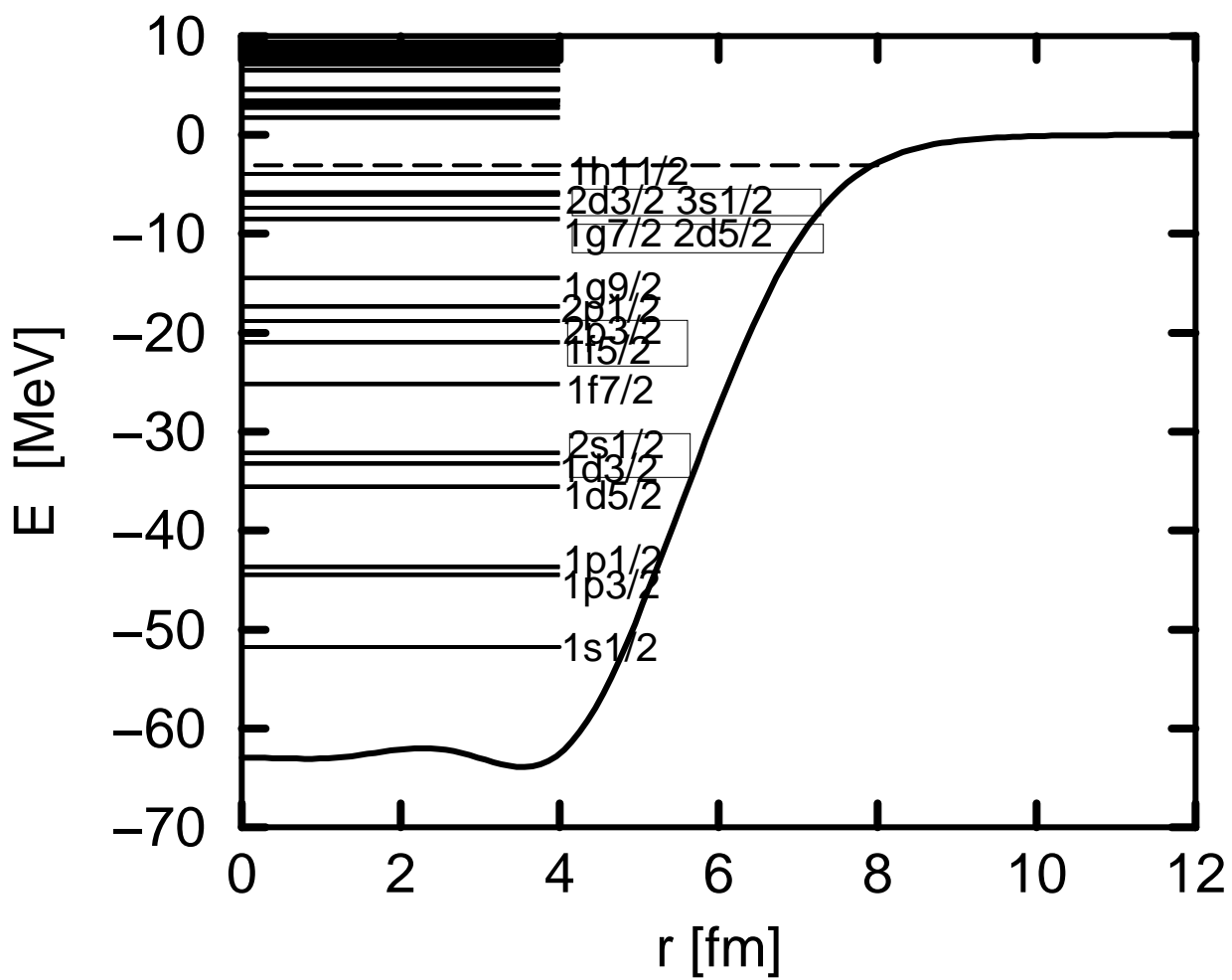
Fig. 5 The comparison of the effective centrifugal barrier (CB) $(E - V)\frac{\kappa(\kappa - 1)}{r^2}$ (dashed lines and dot-dashed lines) and the effective pseudo-spin orbital potential (PSOP) $\frac{\kappa}{r} \frac{dV}{dr}$ (solid line) multiplied by the square of the wave function F of the lower components in arbitrary scale for $d_{3/2}$ (upper) and $s_{1/2}$ (lower) in ^{120}Zr . The dashed lines are for $1d_{3/2}$ and $2s_{1/2}$, and the dot-dashed lines are for $2d_{3/2}$ and $3s_{1/2}$.

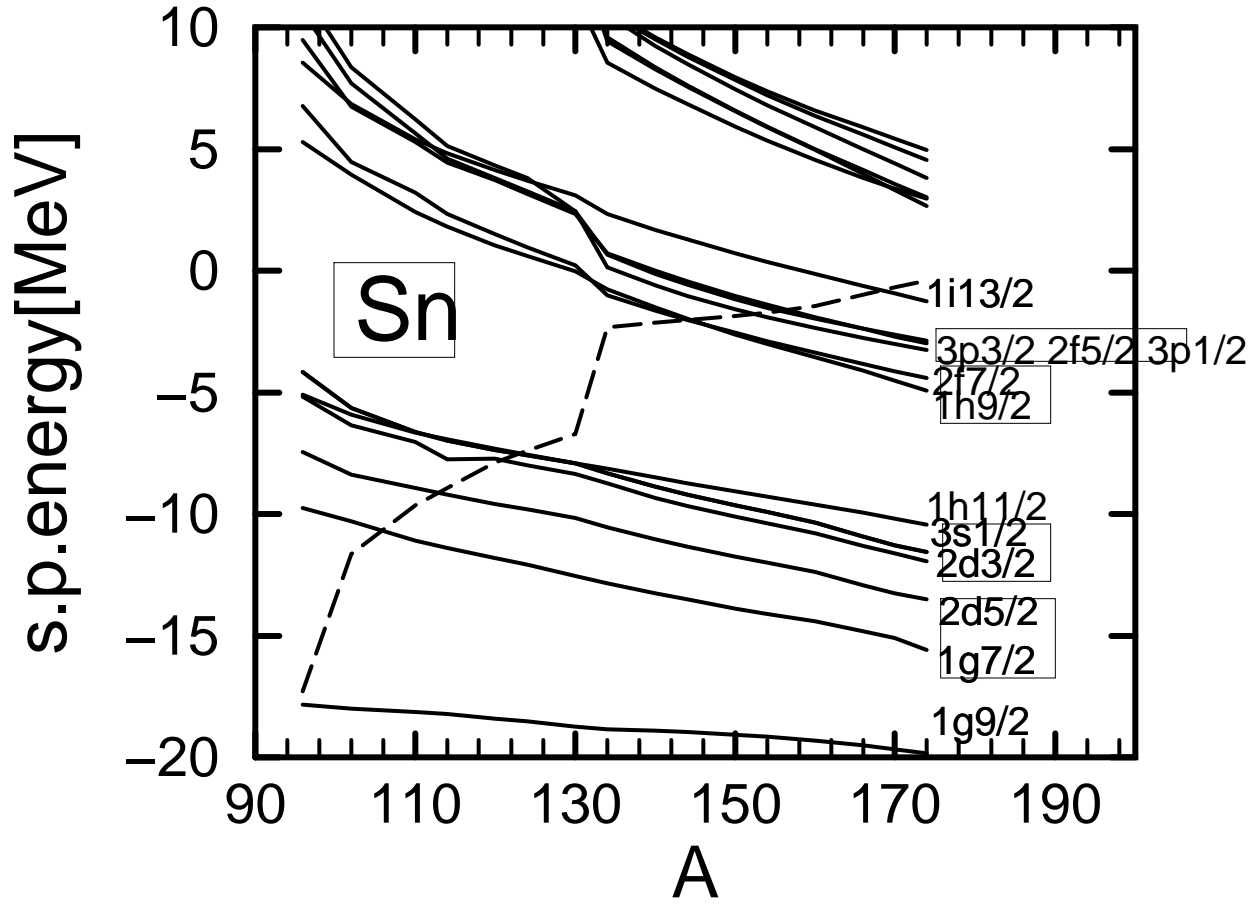
Fig. 6 The upper component G and lower component F of the Dirac wave functions for the pseudo-spin partners in ^{120}Zr . The phase of the Dirac wave functions for one of the pseudo-spin partners has been reversed in order to have a careful comparison.

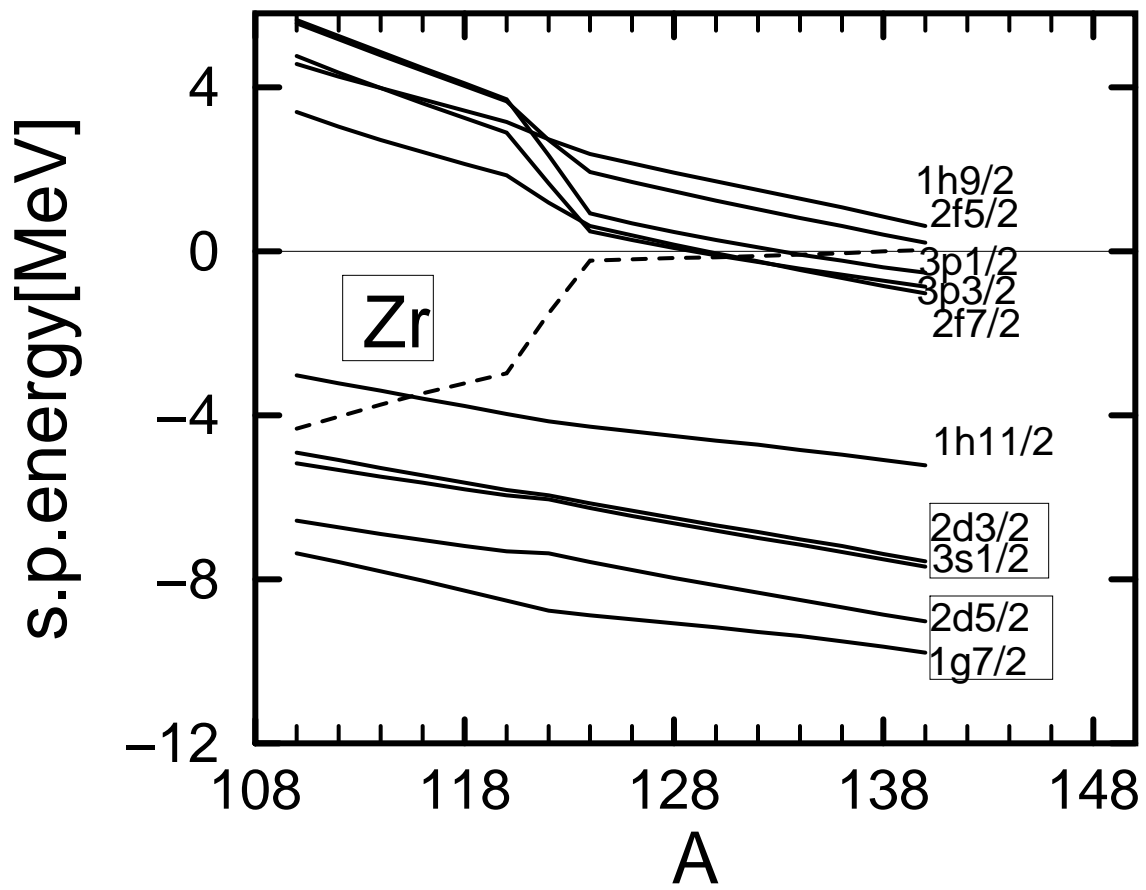
^{150}Sn Neutron

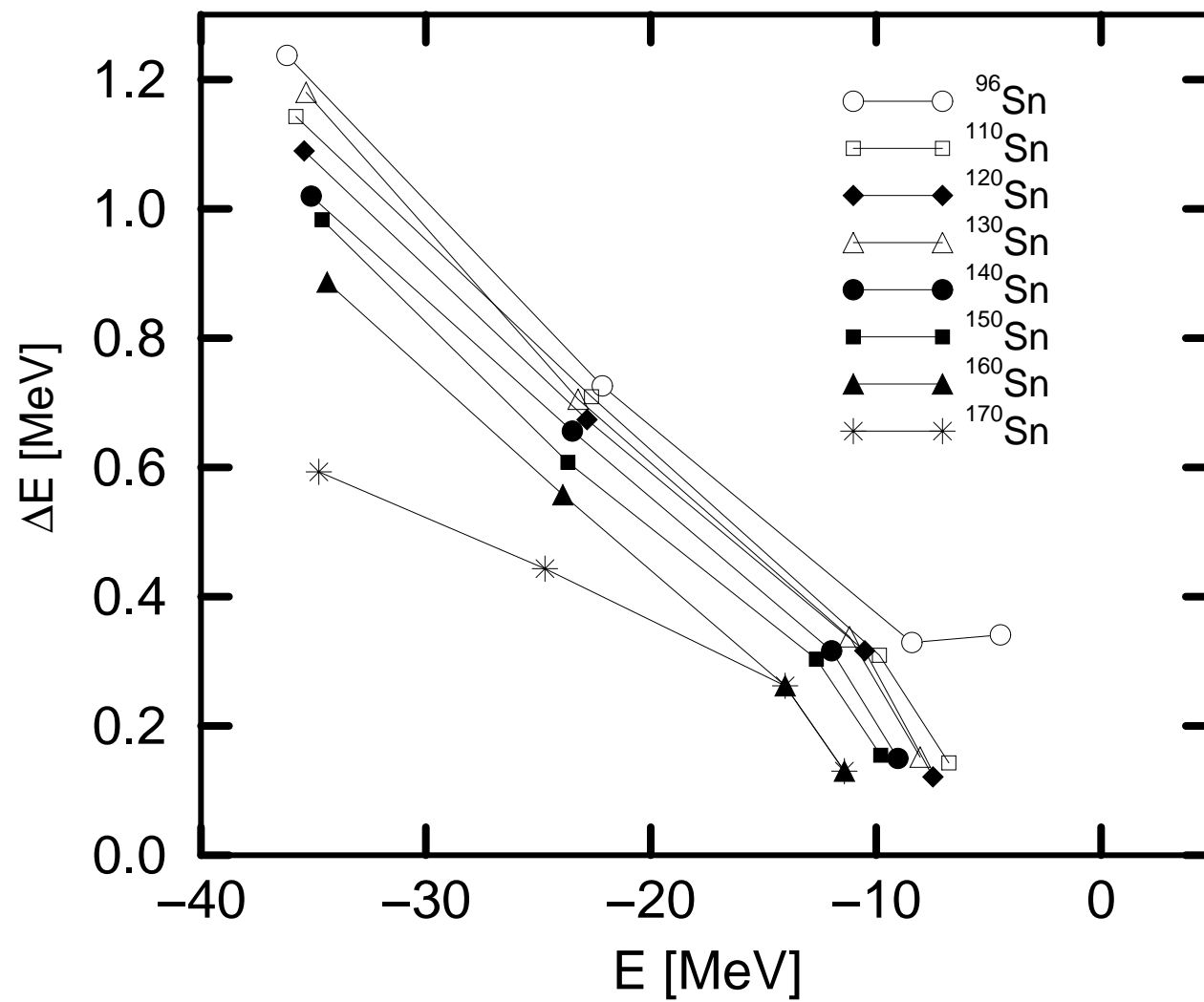


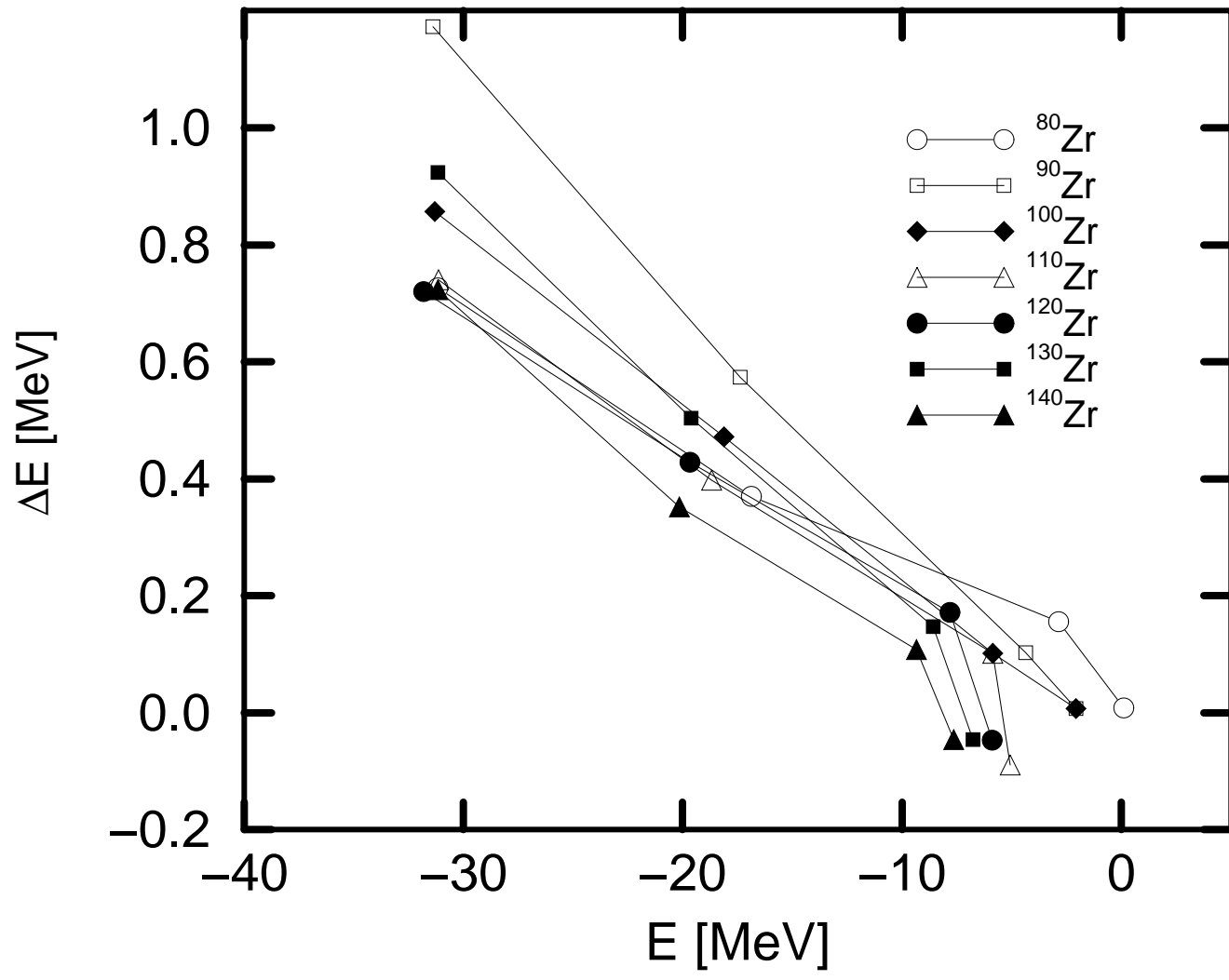
^{120}Zr Neutron

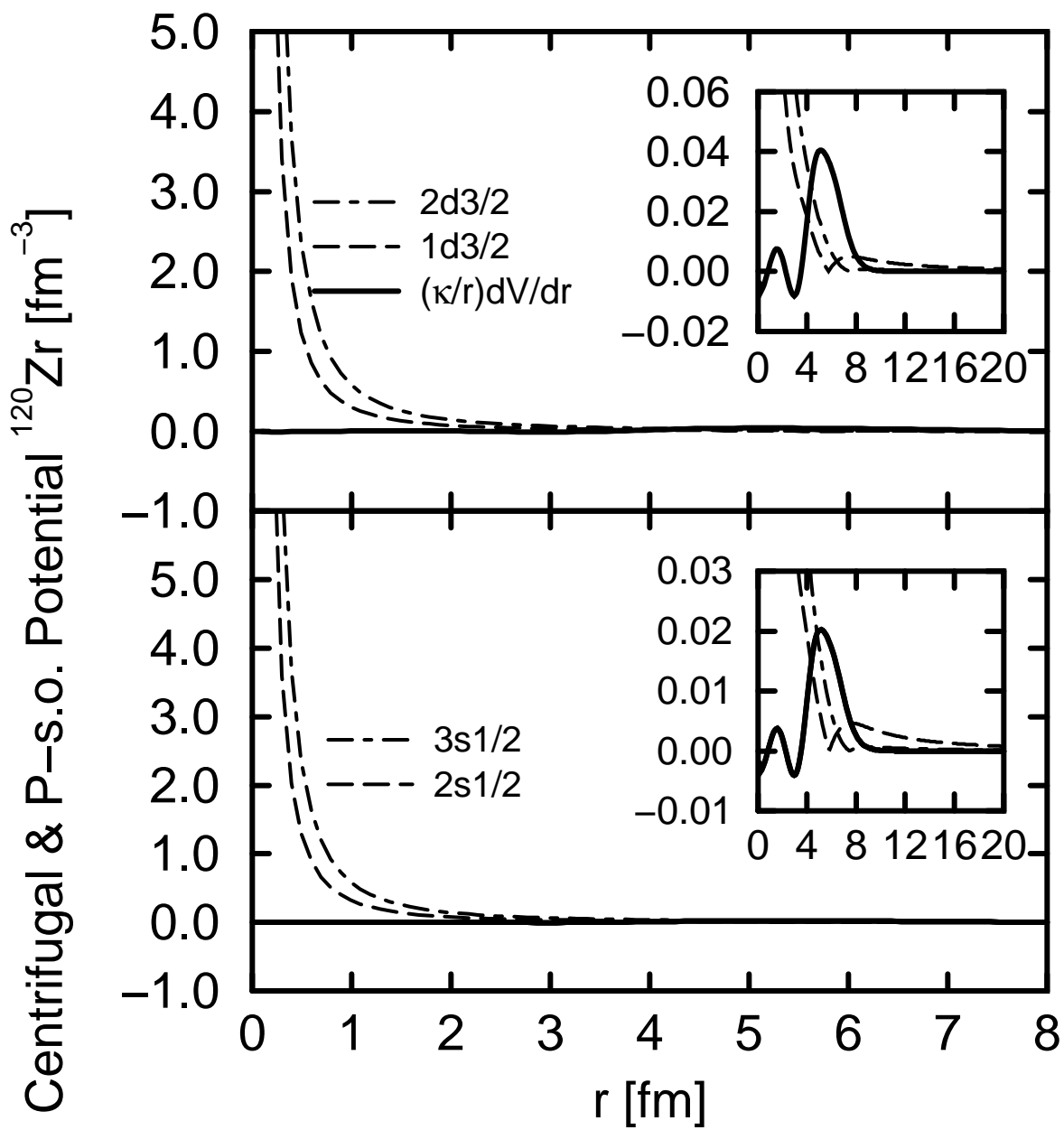


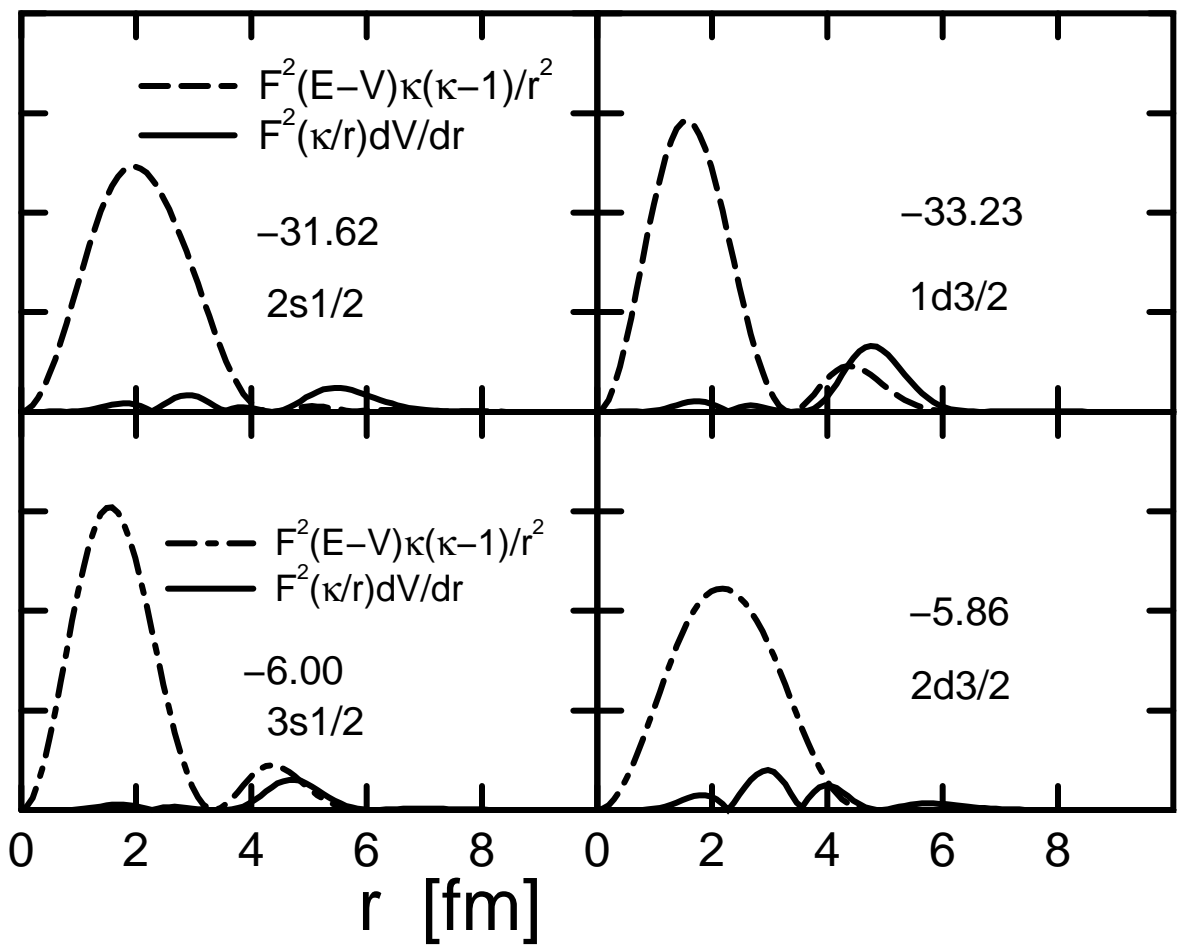












Wave function for Pseudo-spin Partners

